

METHOD FOR ACCURACY ASSESSMENT OF TOPO-BATHYMETRIC SURFACE MODELS BASED ON GEOSPATIAL DATA RECORDED BY UAV AND USV VEHICLES

Oktawia Lewicka^{1,2)}

1) Department of Geodesy and Oceanography, Gdynia Maritime University, ul. Morska 81-87, 81-225 Gdynia, Poland
(✉ o.lewicka@wn.umg.edu.pl,)

2) Marine Technology Ltd., ul. Wiktora Roszczyńskiego 4-6, 81-521 Gdynia, Poland

Abstract

Geospatial data obtained using Unmanned Aerial Vehicles (UAVs) and Unmanned Surface Vehicles (USVs) are increasingly used to model the terrain in the coastal zone, in particular in shallow waterbodies (with a depth of up to 1 m). In order to generate a terrain relief, it is important to choose a method for modelling that will allow it to be accurately projected. Therefore, the aim of this article is to present a method for accuracy assessment of topo-bathymetric surface models based on geospatial data recorded by UAV and USV vehicles. Bathymetric and photogrammetric measurements were carried out on the waterbody adjacent to the public beach in Gdynia (Poland) in 2022 using a DJI Phantom 4 RTK UAV and an AutoDron USV. The geospatial data integration process was performed in the Surfer software. As a result, Digital Terrain Models (DTMs) in the coastal zone were developed using the following terrain modelling methods: Inverse Distance to a Power (IDP), Inverse Distance Weighted (IDW), kriging, the Modified Shepard's Method (MSM) and Natural Neighbour Interpolation (NNI). The conducted study does not clearly indicate any of the methods, as the selection of the method is also affected by the visualization of the generated model. However, having compared the accuracy measures of the charts and models obtained, it was concluded that for this type of data, the kriging (linear model) method was the best. Very good results were also obtained for the NNI method. The lowest value of the Root Mean Square Error (RMSE) (0.030 m) and the lowest value of the Mean Absolute Error (MAE) (0.011 m) were noted for the GRID model interpolated with the kriging (linear model) method. Moreover, the NNI and kriging (linear model) methods obtained the highest coefficient of determination value (0.999). The NNI method has the lowest value of the R68 measure (0.009 m), while the lowest value of the R95 measure (0.033 m) was noted for the kriging (linear model) method.

Keywords: terrain modelling, coastal zone, geospatial data, Unmanned Aerial Vehicle (UAV), Unmanned Surface Vehicle (USV).

© 2023 Polish Academy of Sciences. All rights reserved

Copyright © 2023. The Author(s). This is an open-access article distributed under the terms of the Creative Commons Attribution-NonCommercial-NoDerivatives License (CC BY-NC-ND 4.0 <https://creativecommons.org/licenses/by-nc-nd/4.0/>), which permits use, distribution, and reproduction in any medium, provided that the article is properly cited, the use is non-commercial, and no modifications or adaptations are made.

Article history: received March 31, 2023; revised April 26, 2023; accepted May 1, 2023; available online September 16, 2023.

1. Introduction

The integration of geospatial data recorded using different devices involves combining measurement results that enable their analysis [1–3]. Each device records data in a different spatial reference system. To analyze the terrain relief, it is necessary to import the recorded data into a uniform spatial reference system [4]. The process of geospatial data harmonization is particularly important in the coastal zone, as it is the most geomorphologically variable area on the Earth. This is due to the continuous influence of the atmosphere, hydrosphere and human activities [5,6].

Bathymetric and topographic measurements in the coastal zone are carried out using hydroacoustic and optoelectronic devices and systems [7,8]. Hydroacoustic methods base their operation on echolocation, which involves sending a high-frequency sound wave deep into the water, followed by recording the vibrations of the wave reflected from the bottom. The main hydroacoustic devices and systems include: a hydrometric station, an *Inertial Navigation System* (INS), a *Multi-Beam Echo Sounder* (MBES), a positioning system *Differential Positioning System* (DGPS) or *Real Time Kinematic* (RTK)), a *Single Beam Echo Sounder* (SBES), a *Sound Navigation and Ranging* (SONAR) and a sound velocity probe [9–14]. Optoelectronic methods use the properties of light to record and process geospatial data, as well as their operation involves the conversion of electric signals into optical signals and vice versa. The main optoelectronic devices and systems include: an *Airborne Lidar Bathymetry* (ALB), an image sensor (a photodiode detector, a photomultiplier tube or *Charge-Coupled Device* (CCD) and *Complementary Metal-Oxide-Semiconductor* (CMOS) cameras, an INS, a laser rangefinder, a positioning system (DGPS or RTK), a *Radio Detection and Ranging* (RADAR) and *Terrestrial Laser Scanning* (TLS) [15–20].

Dąbrowski *et al.* [21] proposed a method for integrating geospatial data acquired using a *Global Navigation Satellite System* (GNSS) RTK receiver, a TLS, an *Unmanned Aerial Vehicle* (UAV) and an *Unmanned Surface Vehicle* (USV). This method was verified based on data recorded during a measurement study conducted in Sopot (Poland) in 2019. It used a DJI Mavic Pro UAV for surveying the land and water area, a GNSS RTK Trimble R10 receiver for validating the method of geospatial data integration and georeferencing images taken by the drone, a HyDrone USV, on which a GNSS RTK receiver and an SBES were mounted, for surveying the water area, as well as a Trimble TX8 laser scanner for surveying the land area. The study demonstrated that the deviation values in the horizontal plane did not exceed 0.016 m, while the deviation values in the vertical plane amounted to a maximum of 0.027 m.

Erena *et al.* [22] developed, in collaboration with companies, a *Remotely Operated Vehicle* (ROV), an UAV and an USV, as well as presented a methodology for the integration of data acquired using unmanned measurement platforms for the bathymetric and topographic monitoring of 21 waterbodies of the Segura River (Spain). The study used a GNSS RTK EMLID Reach RS receiver, a SIBIU-IMIDA ROV (comprising an Airmar DST 700 SBES and a 3DR receiver), UAVs (Droning D-650 and D-820), on which a Sony QX1 photogrammetric camera was mounted and a Mambo-IMIDA USV equipped with an Airmar 50/200 kHz SBES. Moreover, *Light Detection and Ranging* (LiDAR) data (Leica ALS50-II Lidar system) were recorded using a manned aerial vehicle. In the first stage, the data acquired using the USV were used to generate a *Digital Surface Model Bathymetry* (DSMB), while the data acquired using the GNSS RTK receiver, LiDAR and the UAV were used to generate a *Digital Surface Model Photogrammetry* (DSMP). This was followed by integrating data on the land and water area, based on which geospatial analyses related to the water volume could be carried out. The study demonstrated that the data acquired using unmanned measurement platforms were characterized by high quality and enabled precise determination of geomorphological changes in waterbodies due to relief-forming processes such as erosion which reduces the capacity of the Segura River waterbodies under study.

Lubczonek *et al.* [23] proposed a method for integrating data acquired using a UAV and a USV. The study aimed to generate a bathymetric chart that included depths all the way to the shoreline. It used a DJI Phantom 4 Pro UAV equipped with a CMOS camera with a resolution of 20 Mpx, a GNSS receiver (positioning accuracy of 0.5–1.5 m) and a Gerris USV on which an Echologer EU400 SBES, a GNSS RTK EMLID Reach M2 receiver and an *Inertial Measurement Unit* (IMU) were mounted. Moreover, *Ground Control Points* (GCP) determined using the GNSS RTK geodetic method were used for the georeferencing of images taken by the drone. The study was conducted on the shallow-water Lake Dąbie (Poland) with an average depth of 2.61 m. The data acquired using unmanned measurement platforms were subjected to a harmonization process to generate a digital model of the waterbody. Five methods were applied for terrain modelling: *Inverse Distance to a Power* (IDP), kriging, *Natural Neighbour Interpolation* (NNI), radial basis function and triangulation. The study demonstrated that the accuracy of modelling the land surface with the above-mentioned methods was high (*Mean Error* (ME) = 0.01 m, *Root Mean Square Error* (RMSE) = 0.03 m). Therefore, the data acquired using unmanned measurement platforms can be used for compiling navigational charts of shallow (coastal) waterbodies, analyzing the seabed shape in the vicinity of hydrotechnical structures, or archaeological mapping.

The literature research has revealed that geospatial data obtained using UAVs and USVs are increasingly used to model the terrain in the coastal zone. Therefore, the aim of writing this article is to present a method for accuracy assessment of topo-bathymetric surface models based on geo-spatial data recorded by UAV and USV vehicles.

This article is structured as follows: Section 2 describes the measurement place. Moreover, this section presents how geospatial data recorded by UAV and USV vehicles were elaborated. In Section 3 *Digital Terrain Models* (DTMs) are presented which were developed using the following terrain modelling methods: IDP, *Inverse Distance Weighted* (IDW), kriging, the Modified Shepard's Method (MSM) and NNI. Then, the accuracy of the generated models was determined. The paper closes with final (general and detailed) conclusions that summarize its content.

2. Materials and Methods

2.1. Topo-bathymetric Data Integration Models

Topo-bathymetric measurements were carried out on the waterbody at the public beach in Gdynia. Three-dimensional coordinates of the underwater area (bathymetric data) were acquired using the AutoDron USV [24, 25]. However, three-dimensional coordinates of the land area (photogrammetric data) were obtained using the DJI Phantom 4 RTK [26].

Topo-bathymetric models were generated based on the bathymetric data derived from the USV and the topographic data recorded by the UAV using the Surfer software [27]. Moreover, this software was also used for integrating bathymetric and topographic data [7], as well as their visualization. The bathymetric data were assigned coordinates from differential GNSS RTK measurements. Initially, the GNSS RTK recorded data in the PL-2000 plane coordinate system and the PL-EVRF2007-NH normal height system. However, for the current study, the plane coordinates from the PL-2000 system were transformed into the PL-UTM system [28]. On the other hand, the UAV point cloud obtained georeferencing from georeference points whose coordinates were derived from differential GNSS RTK measurements. It should be mentioned that the control points derived from the GNSS RTK receiver were originally recorded in the PL-2000 and PL-EVRF2007-NH systems. Therefore, it was reasonable to carry out the transformation of control point plane coordinates. An .xyz file was then generated from the UAV point cloud

using the Pix4D software. It is worth noting that only the beach was used to generate the topobathymetric model. In summary, the process of preparing bathymetric and topographic data involved the transformation of georeference points needed for the performance of georeferencing of the UAV cloud and bathymetric data into the common plane coordinate system (PL-UTM).

The next model generation stage was based on the visualization of the interpolated model data. The interpolated values are presented as either GRID or *Triangulated Irregular Network* (TIN) models. For the Surfer software, it is the GRID model, *i.e.*, a grid of squares whose nodal points have specified terrain surface heights. The data prepared for the model were derived from two different devices. The UAV provided 28,990 points for the narrow strip of the beach, while the USV provided 5136 points. The GRID network for all the models was generated with a spacing of 1 m for the X-axis and 1 m for the Y-axis, and the number of rows and columns was 412×213 . Thus, the total number of nodes for each generated GRID network was 87,756. However, it should be noted that not every method allowed information on depths and heights in all squares to be obtained.

Following the generation of the GRID network, the statistical parameters for individual Digital Terrain Models of the GRID type were calculated: Root Mean Square (m), minimum and maximum interpolated value (m), range (R) (m) and *InterQuartile Range* (IQR) (m):

$$\text{RMS} = \sqrt{\frac{\sum_i^n \hat{z}_i^2}{n}}, \quad (1)$$

$$R = \max(\hat{z}) - \min(\hat{z}), \quad (2)$$

$$\text{IQR} = Q_3(\hat{z}) - Q_1(\hat{z}), \quad (3)$$

where:

- n – number of measurement points (–);
- i – numbering representing successive measurement points (–);
- z_i – height of the i -th point measured by the UAV and USV vehicles (m);
- \hat{z}_i – interpolated value of z_i (m);
- $\max(\hat{z})$ – maximum value of \hat{z} (m);
- $\min(\hat{z})$ – minimum value of \hat{z} (m);
- $Q_1(\hat{z})$ – the first quartile (25th empirical quartile) of the \hat{z} value (m);
- $Q_3(\hat{z})$ – the third quartile (75th empirical quartile) of the \hat{z} value (m).

In order to assess the accuracy of each interpolated point cloud, it was then decided to compare the generated height values with the height values recorded by the UAV and USV vehicles with the same plane coordinates based on the model accuracy measures: RMSE (m) [29], *Mean Absolute Error* (MAE) (m) [30] and the coefficient of determination (R^2) (–) [31]:

$$\text{RMSE} = \sqrt{\frac{\sum_i^n (\hat{z}_i - z_i)^2}{n}}, \quad (4)$$

$$\text{MAE} = \frac{\sum_i^n |\hat{z}_i - z_i|}{n}, \quad (5)$$

$$R^2 = \frac{\sum_i^n (\hat{z}_i - \bar{z})^2}{\sum_i^n (z_i - \bar{z})^2}, \quad (6)$$

where: \bar{z} – arithmetic mean of the z value (m).

Moreover, the measurement results are presented using the commonly applied statistical position accuracy measures: R68 (m) and R95 (m) [32] for the differences between the height coordinates measured by the UAV and USV and the modelled height coordinates. These measures were applied because they do not assume normal distribution.

2.2. Method for Accuracy Assessment of Topo-bathymetric Surface Models Based on Geospatial Data Recorded by UAV and USV Vehicles

The method for accuracy assessment of topo-bathymetric surface models based on geospatial data recorded by UAV and USV vehicles (Fig. 1) begins from the collection data stage. Bathymetric

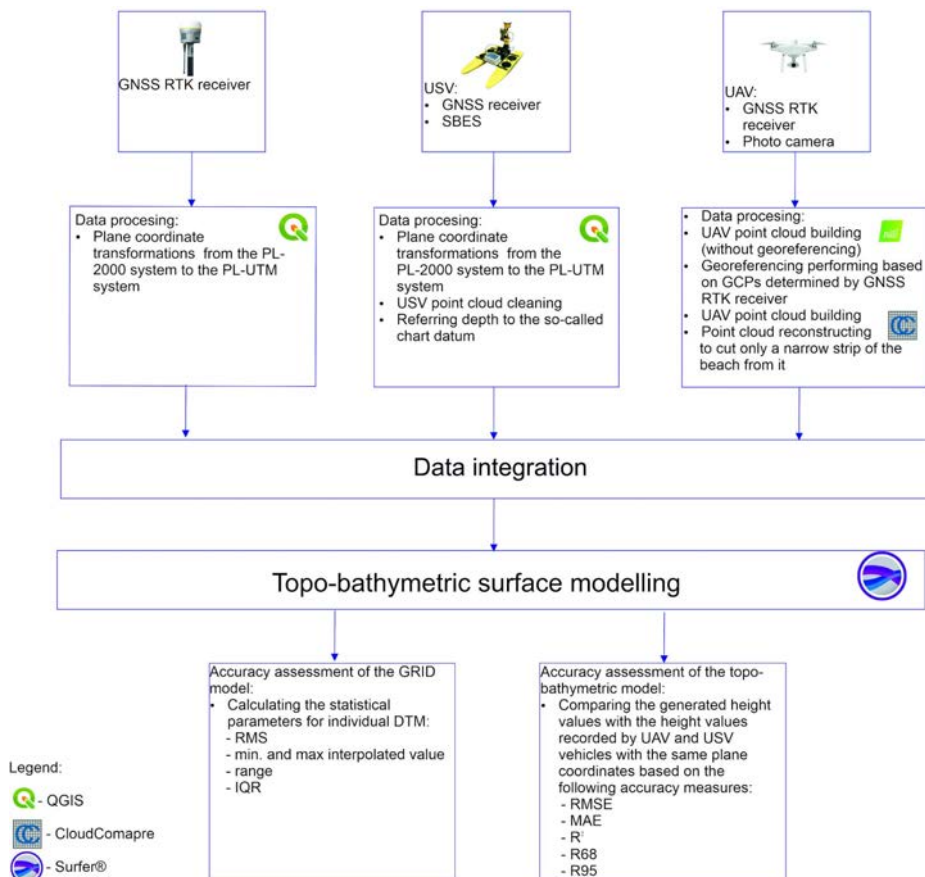


Fig. 1. A flowchart of the method for accuracy assessment of topo-bathymetric surface models based on geospatial data recorded by the UAV and USV vehicles.

data were obtained using the AutoDron USV, while photogrammetric data were recorded using the DJI Phantom 4RTK UAV. Moreover, the course of the shoreline and georeference points needed for the performance of georeferencing were determined with the use of the GNSS RTK receiver. Subsequently, data from the above-mentioned devices were processed.

Processing data which came from the GNSS RTK receiver is based on the transformation of plane coordinates from the PL-2000 system to the PL-UTM system in the QGIS software. Data from the GNSS RTK receiver included the course of the shoreline and coordinates of georeferencing points.

The development of bathymetric data is a multi-stage process and requires a very thorough check of the data. At the beginning, transformations of plane coordinates from the PL-2000 system to the PL-UTM system were carried out. In the case of the data collected during the measurement study, there was no need to convert the height coordinates. Nevertheless, the coordinate transformation step can be omitted if there are no such requirements. Subsequently, the depths erroneously recorded by the SBES were removed. Finally, the depths were referred to the so-called chart datum. All stages of work in the development of bathymetric data were carried out in the QGIS software.

The development of photogrammetric data began with their being inserted into the Pix4D software. The next stage of work consisted in generating a UAV point cloud. The UAV point cloud was generated in the form of the GRID Digital Surface Model with a grid spacing of 1 m. Subsequently, the process of georeferencing was launched. It was conducted based on georeference points recorded by the GNSS RTK receiver. Then the UAV point cloud was recreated in the CloudCompare software to cut out only the beach and saved in a .csv file.

After the preparation of three measurement data sets (GNSS RTK, UAV and USV), they were combined into one .csv file. Next, the integrated data were inserted into the Surfer software. This program made it possible to generate topo-bathymetric models using the following terrain modelling methods: IDW, IDP ($p = 1$), IDP ($p = 2$), MSM, NNI, kriging (logarithmic model) and kriging (linear model). After generating the GRID model, statistical parameters were calculated for individual DTMs: RMS, minimum and maximum interpolated values, R and IQR.

Then, in order to assess the accuracy of each interpolated point cloud, it was decided to compare the generated height values with the height values recorded by devices with the same plane coordinates based on the following accuracy measures: RMSE, MAE, R^2 , R68 and R95. This is the most important stage in accuracy assessment of topo-bathymetric surface models. However, making a correct accuracy assessment depends on the data preparation process.

3. Results

For the purposes of the research, it was decided to develop DTMs based on the following terrain modelling methods: IDW, IDP ($p = 1$), IDP ($p = 2$), MSM, NNI, kriging (logarithmic model) and kriging (linear model). Only then was it possible to determine statistical parameters for individual DTMs, such as: RMS, R, IQR, RMSE, MAE and R^2 .

3.1. IDW

The IDW was the first interpolation method applied to the data from the measurement study conducted in Gdynia. This method had already been used to interpolate similar data for publication purposes [33,34]. However, only bathymetric data were used for modelling the waterbody adjacent to the beach in Sopot. The modelled waterbody in Sopot faithfully represented the surfaces.

Therefore, it was decided to test the method on the bathymetric and topographic data covering the public beach in Gdynia, which is located close to the beach in Sopot.

The RMS value of heights interpolated with the IDW method was 0.947 m. The minimum height value amounted to 0.006 m, while the maximum value was 1.502 m. The range amounted to 1.496 m, while the IQR was 0.351 m.

The accuracy of the interpolated DTM (Figure 2) in relation to the measurements was determined using the RMSE to be 0.631 m and the MAE to be 0.466 m. The RMSE and MAE values indicate a significant difference between the interpolated and the measurement values. The coefficient of determination was obtained at a level of 0.945, which means that the fit of the model to the measurement data is not satisfactory. The difference between the interpolated value and the measurement value for the R68 measure is 0.492 m, while for the R95 measure, it has a value of 1.451 m.

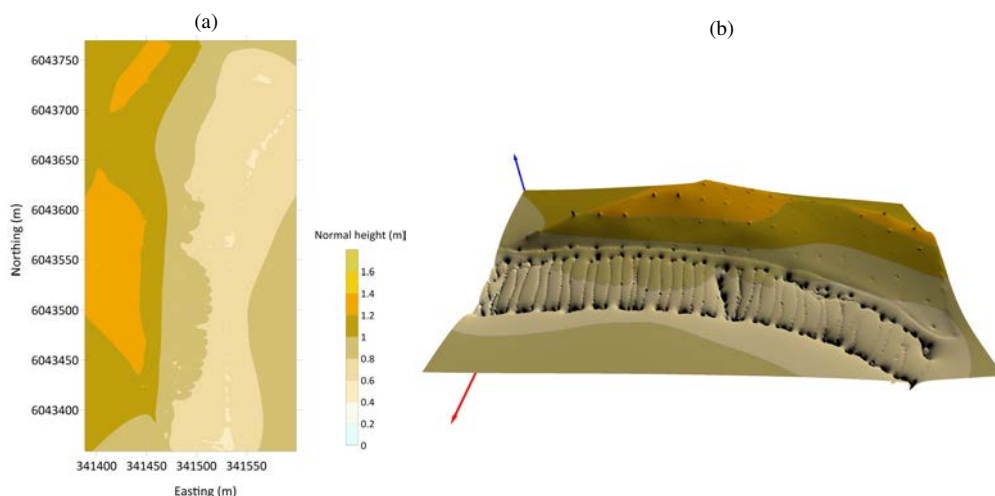


Fig. 2. A topo-bathymetric chart of the waterbody adjacent to the public beach in Gdynia obtained using the IDW method (a) and its 3D visualization (b).

The data prepared for the model were derived from two different devices. The UAV provided 28,990 points of the beach, while the USV provided 5136 points. The bathymetric data covered a larger area. However, it was the topographic data that had a significant effect on the value of interpolated points, which is due to the volume of topographic data. The greater number of UAV points resulted in the USV values having a lesser influence on the interpolated value. Based on the analysis, it can be concluded that the application of the IDW method for a large data set with unevenly distributed measurement points can result in an incorrect surface representation.

3.2. IDP ($p = 1$)

Another method that should be tested on the bathymetric and topographic data is the IDP. In the literature, the method is also known as the IDW method modified by the exponent parameter [35].

The RMS value of heights interpolated with the IDP ($p = 1$) method was 1.263 m. The minimum height value amounted to -1.332 m, while the maximum value was 2.690 m. The range amounted to 4.022 m, while the IQR was 2.494 m.

The accuracy of the interpolated DTM (Fig. 3) in relation to the measurements was determined using the RMSE to be 0.058 m and the MAE to be 0.024 m. The coefficient of determination was obtained at a level of 0.998, which means that the fit of the model to the measurement data is very good. The difference between the interpolated value and the measurement value for the R68 measure is 0.020 m, while for the R95 measure, it has a value of 0.072 m.

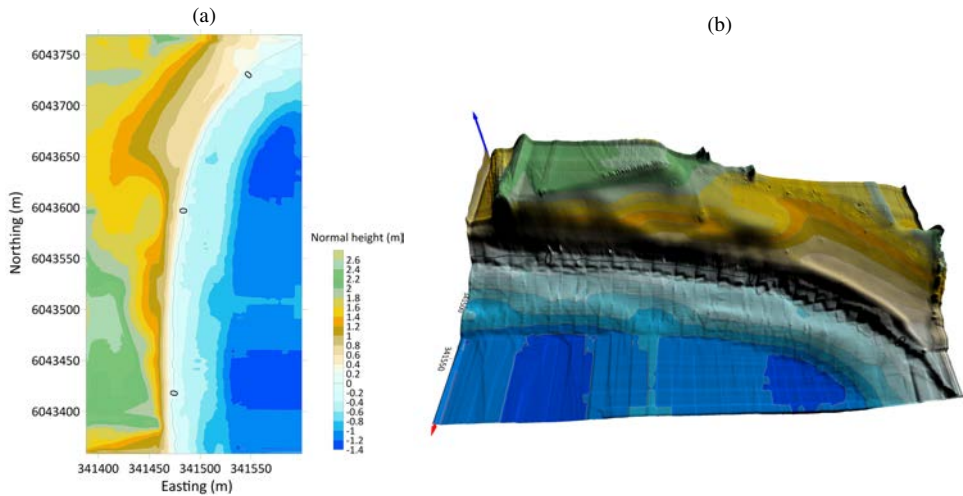


Fig. 3. A topo-bathymetric chart of the waterbody adjacent to the public beach in Gdynia, obtained using the IDP ($p = 1$) method (a) and its 3D visualization (b).

Limiting the maximum number of points involved in interpolating a particular point is especially important when handling data derived from two independent devices, especially when there are significantly more UAV data than the data measured by the SBES. Nevertheless, it should be expected that it will not always be possible to correctly determine the maximum number of points that will affect the calculation of the values of interpolated points.

3.3. IDP ($p = 2$)

Another analysis was performed on the IDP method using the power exponent as a function of weight [36, 37]. Usually, a basic exponent value of $p = 2$ or $p = 3$ is applied. However, it should be noted that considering the exponent p in the IDP method does not always result in the representation of the actual surface.

Since the application of the IDP method with the parameter $p = 1$ and taking into account the range of data with a preset radius yielded a very good fit, it was decided to consider the same method but with a different parameter p . For this case of the IDP method, the parameter p has a value of 2, while the data range was determined to be the same as for the previous IDP ($p = 1$) method.

The RMS value of heights interpolated with the IDP ($p = 2$) method was 1.262 m. The minimum height value amounted to -1.346 m, while the maximum value was 3.102 m. The range amounted to 4.448 m, while the IQR was 2.488 m.

The accuracy of the interpolated DTM (Fig. 4) in relation to the measurements was determined using the RMSE to be 0.041 m and the MAE to be 0.016 m. The coefficient of determination

was obtained at a level of 0.999, which means that the fit of the model to the measurement data is very good. The difference between the interpolated value and the measurement value for the R68 measure is 0.013 m, while for the R95 measure, it has a value of 0.046 m.

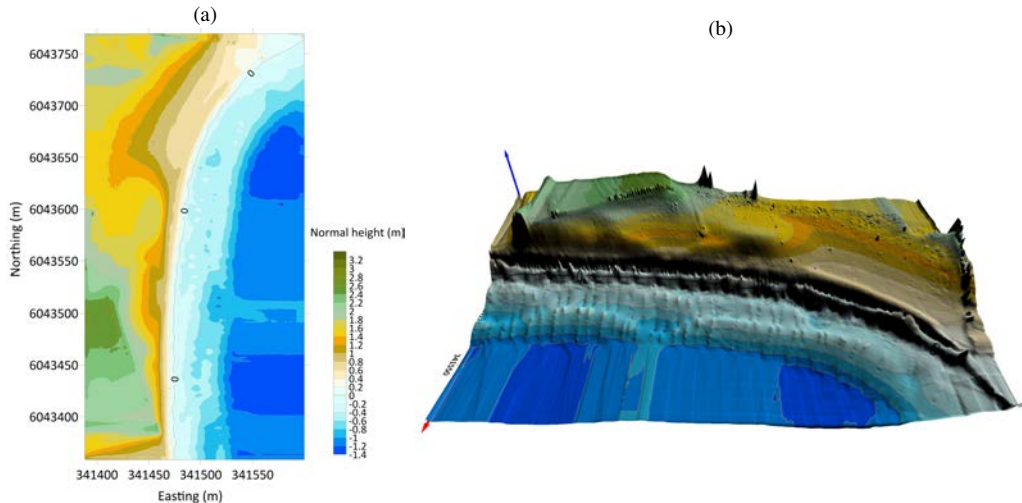


Fig. 4. A topo-bathymetric chart of the waterbody adjacent to the public beach in Gdynia, obtained using the IDP ($p = 2$) method (a) and its 3D visualization (b).

Based on the conducted comparative analysis of two IDP models, it can be concluded that increasing the parameter does not affect the interpolated values significantly. Moreover, the visualization of data using the IDP ($p = 1$) and IDP ($p = 2$) methods is similar because the interpolated values of both methods are comparable.

3.4. MSM

Another method applied to the integrated data is MSM [38–40]. This method is particularly dedicated to interpolating a small data set, which is confirmed by the publication [39]. Given the scarcity of studies that interpolate integrated data using the MSM method, it was decided to apply this method to interpolate the data from the measurement study conducted in Gdynia.

The GRID model generated using the MSM method was obtained, assuming that the two radii needed for defining the ellipse have a value of 42.1 m. However, the number of points in each ellipse is 13, while the number of points needed for the determination of weight coefficients is 19. The generated GRID model did not cover all the squares in the grid with data. A total of 55,946 nodes contained interpolated values, while data was missing at as many as 31,810 nodes. On the other hand, the RMS value of heights interpolated with the MSM method was 1.495 m. The minimum height value amounted to -1.370 m, while the maximum value was 3.857 m. The range amounted to 5.227 m, while the IQR was 2.060 m.

A comparative analysis of the interpolated values and the measurement values for the MSM method was conducted on 34,106 points, which is due to the fact that the entire model area was not covered with values. The accuracy of the interpolated DTM (Fig. 5) in relation to the measurements was determined using the RMSE to be 0.104 m and the MAE to be 0.022 m. The coefficient of determination was obtained at a level of 0.992, which means that the fit of the model

to the measurement data is not satisfactory. The difference between the interpolated value and the measurement value for the R68 measure is 0.009 m, while for the R95 measure, it has a value of 0.070 m.

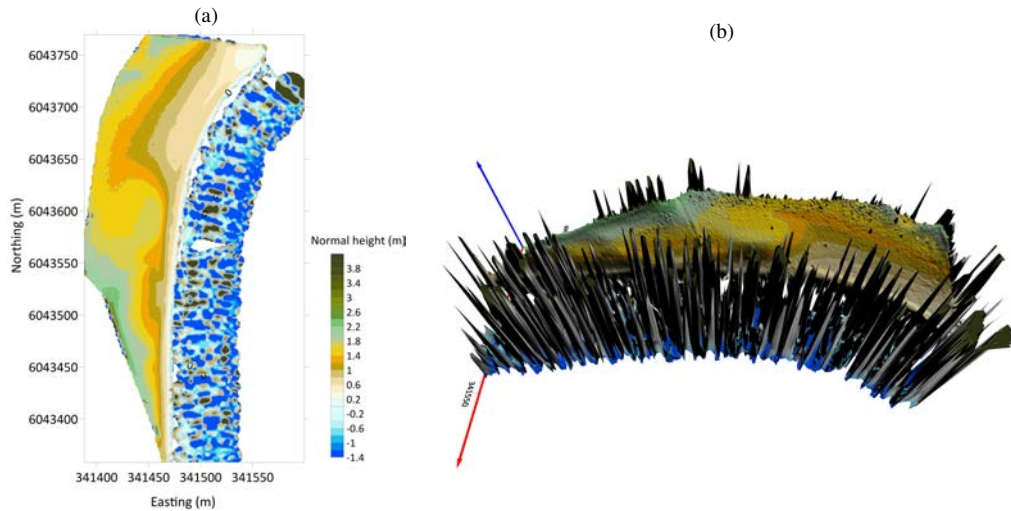


Fig. 5. A topo-bathymetric chart of the waterbody adjacent to the public beach in Gdynia, obtained using the MSM method (a) and its 3D visualization (b).

As can be seen, the MSM model was not generated for the waterbody adjacent to the public beach in Gdynia. The areas not covered with data are located at locations that were not overlapped with measurement data or where their number was insufficient. These are located at the interface between land and water. Based on the conducted analysis, it can be concluded that the MSM method is not suitable for unevenly distributed data.

3.5. NNI

Another method implemented on the UAV and USV data is the NNI method [41]. This method is most commonly used in geology [42]. However, it performs very well for the interpolation of evenly distributed data. It is also applied where a lack of data occurs in regularly distributed data. Therefore, it was decided to apply the NNI method for data integration. The surface of the waterbody adjacent to the public beach in Gdynia, including the narrow strip of the beach, is densely covered with points. On the other hand, in certain places, there is a lack of data.

As with the MSM method, the grid of squares created with the NNI method did not contain height data at each node. A total of 61927 nodes only contained data, while 25829 nodes lacked data. This is due to the properties of the model that is mainly based on the creation of a triangle network with the Voronoi method, which is created locally in relation to the interpolating points. This means that the interpolated values are not created at the edges of the interpolated area. The RMS value of heights interpolated with the NNI method was 1.120 m. The minimum height value amounted to -1.365 m, while the maximum value was 3.418 m. The range amounted to 4.783 m, while the IQR was 2.036 m.

The accuracy of the interpolated DTM (Fig. 6) in relation to the measurements was determined using the RMSE to be 0.031 m and the MAE to be 0.011 m. The coefficient of determination

was obtained at a level of 0.999, which means that the fit of the model to the measurement data is very good. The difference between the interpolated value and the measurement value for the R68 measure is 0.009 m, while for the R95 measure, it has a value of 0.034 m.

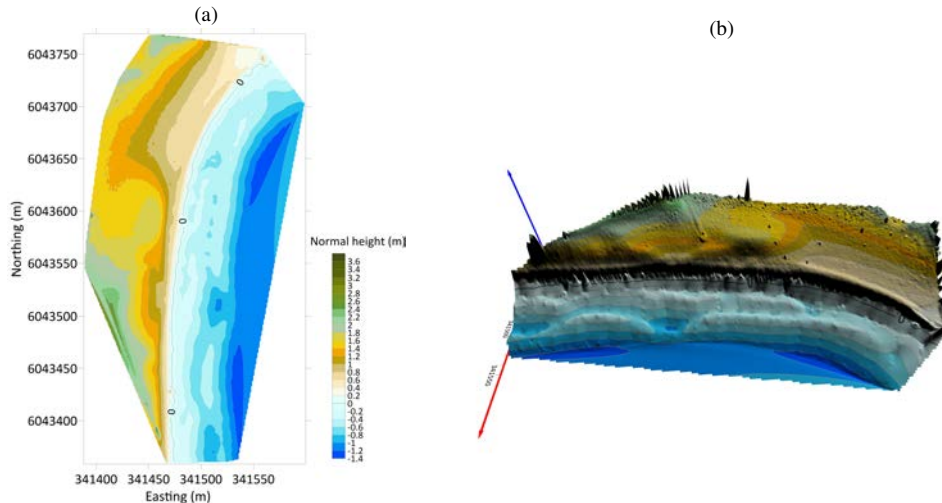


Fig. 6. A topo-bathymetric chart of the waterbody adjacent to the public beach in Gdynia, obtained using the NNI method (a) and its 3D visualization (b).

The GRID model covers a much smaller area than the previous models. The NNI method prevents the generation of a network for areas not covered with data. However, its application to integrated data allowed for a very good fit of the model with respect to the measurement data measured by two independent devices.

3.6. Kriging (Logarithmic Model)

The kriging method is among the most effective terrain modelling methods [43, 44]. This method, similar to the IDW methods, assigns greater weights to the points located closer to the interpolated point. However, in contrast to the IDW method, the weights are determined based on a semivariogram.

The modelling of a semivariogram involves the selection of a mathematical function to most accurately describe the empirical model. According to the calculations for 100 points, the best model for the data under analysis was a logarithmic model. A radius specifying the range for the interpolated point was then defined. The adopted values were the same as those for the previous methods. It should be noted that with a greater number of points in the ellipse, assuming a limited number of points in a particular ellipse, the points that are closest to the interpolated point are selected. The interpolation yielded a grid with a total number of 87,756 nodes. The RMS value of heights interpolated with the kriging (logarithmic model) method was 1.381 m.

The minimum height value amounted to -1.370 m, while the maximum value was 3.857 m. The range amounted to 5.227 m, while the IQR was 2.486 m. The accuracy of the interpolated DTM (Fig. 7) in relation to the measurements was determined using the RMSE to be 0.604 m and the MAE to be 0.331 m. The coefficient of determination was obtained at a level of 0.793 , which means that the fit of the model to the measurement data is not satisfactory. The high value

of the RMSE and MAE measures, as well as the low value of the coefficient of determination indicate that the kriging method was not the best for the interpolation of a large volume of data. This was also confirmed by the position measures. The difference between the interpolated value and the measurement value for the R68 measure is 0.275 m, while for the R95 measure, it has a value of 1.428 m.

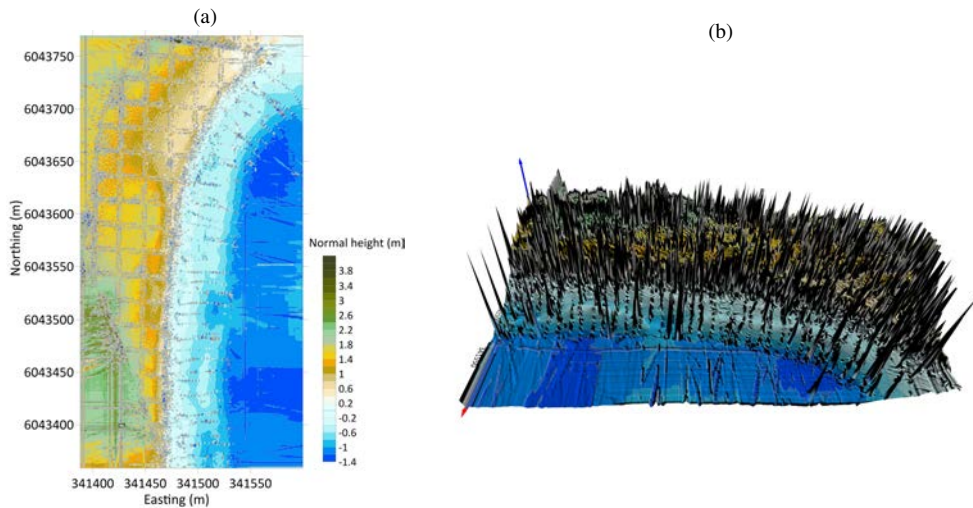


Fig. 7. A topo-bathymetric chart of the waterbody adjacent to the public beach in Gdynia, obtained using the kriging (logarithmic model) method (a) and its 3D visualization (b).

The topo-bathymetric chart shows the values of the depths and heights of the waterbody adjacent to the beach, including the narrow strip of the beach. However, small areas in the form of squares or other geometric figures are noticeable on the map. Since the interpolated surface is not smooth, smoothing with the spline method should be applied.

3.7. Kriging (Linear Model)

The results of the GRID model created with the kriging method were determined by the selection of the semivariogram model. Therefore, it was decided to apply the kriging method to the same data but using a different semivariogram model. The kriging method with a logarithmic semivariogram failed to yield a very good fit of the model against the measurement data. Hence, the linear model of the semivariogram was applied, as it is used by default. What is more, its application in the kriging model enabled the generation of a very accurate model of the interpolated surface. The other variables for the model remained the same as for the kriging (logarithmic model) method.

The RMS value of heights interpolated with the kriging (logarithmic model) method was 1.302 m. The minimum height value amounted to -1.445 m, while the maximum value was 3.902 m. The range amounted to 5.347 m, while the IQR was 2.500 m.

The accuracy of the interpolated DTM (Fig. 8) in relation to the measurements was determined using the RMSE to be 0.030 m and the MAE to be 0.011 m. The coefficient of determination was obtained at a level of 0.999, which means that the fit of the model to the measurement data is

very good. The difference between the interpolated value and the measurement value for the R68 measure is 0.009 m, while for the R95 measure, it has a value of 0.033 m.

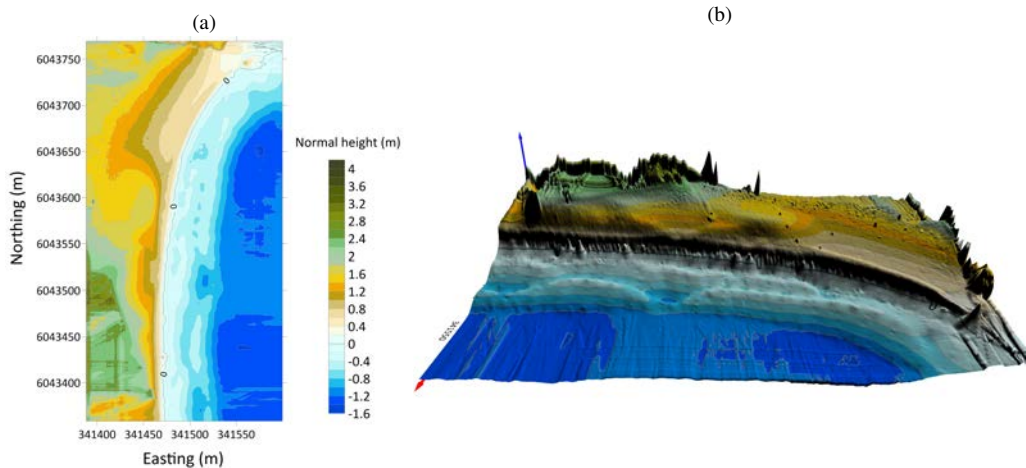


Fig. 8. A topo-bathymetric chart of the waterbody adjacent to the public beach in Gdynia, obtained using the kriging (linear model) method (a) and its 3D visualization (b).

As can be noted, the surface is devoid of sharp contours. Depth differences are visible across the waterbody.

4. Discussion

The rapid development of measurement devices and systems has broadened the horizons for the acquisition and processing of height and depth data in the coastal zone. However, with the development of measurement techniques, the problem of integrating hydroacoustic and optoelectronic data acquired from different devices has emerged [45]. Moreover, another problem worth addressing is the selection of an appropriate method to build a terrain model faithfully representing land using heterogeneous data [46, 47].

Terrain modelling using integrated data is a serious research problem that should be investigated in detail. Therefore, the author of the article decided to generate seven different DTMs based on integrated UAV and USV data. Particularly noteworthy is the fact that the data cover the waterbody adjacent to the public beach in Gdynia, along with a narrow strip of the beach.

The DTMs were generated using different methods. What is more, the IDP and kriging methods were applied twice using different variables, while the models were created in the form of regular grids of squares. Each generated grid of squares comprised 87,756 nodal points, which had specific depths or heights. Table 1 provides a summary of essential information on the GRID-generated models.

The maximum value of the height coordinate in the GRID model was noted for the kriging (linear model) method. However, the minimum value of the depth coordinate was observed for the kriging (linear model) method. It is noteworthy that the model generated with the IDW method contained no negative values, which is due to the properties of the model and the preponderance of the UAV data. More points from the UAV cause the values from the USV to have a significant

Table 1. A summary of information on the GRID-generated models.

Statistical measure (m)	IDW	IDP ($p = 1$)	IDP ($p = 2$)	MSM	NNI	Kriging (logarithmic model)	Kriging (linear model)
h_{\max}^1	1.502	2.690	3.102	3.857	3.418	3.857	3.902
h_{\min}^2	0.006	-1.332	-1.346	-1.370	-1.365	-1.370	-1.445
RMS	0.947	1.263	1.262	1.495	1.120	1.381	1.302
R	1.496	4.022	4.448	5.227	4.783	5.227	5.347
IQR	0.351	2.494	2.448	2.060	2.063	2.486	2.500

The maximum ¹ and minimum ² value of the height coordinate in the GRID model.

impact on the interpolated value. It can be presumed that the IDW method is not suitable to be applied to unevenly distributed data, *i.e.*, where data located in a specific part of the area under study predominate. Having analyzed, for each model, the differences between the highest and the lowest height value in the set, it was concluded that the least varied interpolated data were found in the GRID model obtained with the IDW method. On the other hand, the most varied height data were obtained for the GRID model of the kriging (linear model) method.

The information presented in this study clearly shows the variation in the interpolated data values depending on the method applied. However, to determine which of the methods applied is the best and should be applied for integrated data covering the land and water area, it was decided to compare the accuracies of selected models obtained with different interpolation methods (Table 2).

Table 2. The accuracies of selected terrain modelling methods based on geospatial data recorded by UAV and USV vehicles in the coastal zone.

Statistical measure (m)	IDW	IDP ($p = 1$)	IDP ($p = 2$)	MSM	NNI	Kriging (logarithmic model)	Kriging (linear model)
RMSE (m)	0.631	0.058	0.041	0.104	0.031	0.604	0.030
MAE (m)	0.466	0.024	0.016	0.022	0.011	0.331	0.011
R^2 (-)	0.945	0.998	0.999	0.992	0.999	0.793	0.999
R68 (m)	0.492	0.020	0.013	0.009	0.009	0.275	0.009
R95 (m)	1.451	0.072	0.046	0.070	0.034	1.428	0.033

Based on Table 2, it can be concluded that the lowest value of the RMSE (0.030 m) was noted for the GRID model interpolated with the kriging (linear model) method. However, the lowest value of the MAE (0.011 m) was obtained for the GRID model interpolated with the NNI and the kriging (linear model) methods. The low value of the MAE can be due to a very good fit between the interpolated values and the measurement values for the land area. Another measure taken into account is the coefficient of determination. The highest coefficient of determination value (0.999) was noted for the IDP ($p = 2$), NNI and the kriging (linear model) methods. Moreover, a range limiting measurement points, which affected the determination of the interpolated point value, was also assessed. The lowest coefficient of determination value (0.793) was obtained for the kriging (logarithmic model) method. The lowest value of the R68 measure (0.009 m) was noted for the MSM and NNI methods, while the lowest value of the R95 measure (0.033 m) was obtained for the kriging (linear model) method.

The study also analyzed the distribution of a random variable, *i.e.*, the differences between the height coordinate measured by the UAV and USV vehicles and the modelled height coordinate. To this end, Easy Fit free software was used, which checks, by means of statistical tests such as the Anderson-Darling test, chi-square test and Kolmogorov-Smirnov test [48–51], whether the distribution of a random variable in the population differs from the assumed theoretical distribution. Then, the program classifies the probability distributions according to the obtained statistics for the particular statistical tests. For the purpose of the study, the most commonly used theoretical distributions in geodesy were applied: Beta, Cauchy, chi-square, exponential, gamma, Laplace, logistic, lognormal, normal, Pareto, Rayleigh, Student's and Weibull [52–55]. It follows from the conducted analyses that the empirical distribution of the differences between the interpolated measurement height values is the most similar to the Cauchy distribution for each statistical test. All tests for individual interpolation methods (excluding IDW) showed consistency of the differences between the interpolated and measurement height values with the Cauchy distribution for a significance level of $\alpha = 0.05$.

Based on the statistical analysis and the visual assessment of the generated surfaces, it can be assumed that the kriging (linear model) method performed the best. The model generated using the kriging (linear model) method yielded very good results for selected accuracy measures. What is more, the generated chart covers the entire area. It is worth noting that the generated isobaths are smoothed. In addition, the interpolated surface contains no contours in the form of a so-called bull's-eye. It should be stressed that the NNI method also yielded very good results for accuracy measures. Due to its algorithm, it does not cover the entire area with the interpolated data. The IDP ($p = 2$) can also be considered a suitable method for modelling integrated data.

The accuracies of selected terrain modelling methods and the review of previous studies indicate that the methodology of data acquisition has an impact on the accuracy of the created models. Lubczonek *et al.* [56] proposed a methodology for creating a bathymetric and topographic surface model using interpolation and geodata reduction techniques. This interpolation method based on datasets with different degrees of spatial data reduction. Lubczonek *et al.* [56] wanted to prove that the best results can be obtained if the dataset will be reduced. However, the research presented in this article indicates that feeding of all the data into the model can give very good results. On the other hand, Genchi *et al.* [57] created a topobathymetry model consisting of a topographic point cloud and a bathymetry model which was generated using a different interpolation method. In this case the best interpolated bathymetry (IDW method), which was aligned to the topography (as reference), showed a RMSE of 0.18 m (on average) and a MAE of 0.05 m. The accuracies are much higher than the model created from data on the waterbody adjacent to the public beach in Gdynia. In addition, the IDW method based on geospatial data recorded in Gdynia does not yield good results. Gesch and Wilson [58] developed a seamless multisource topographic/bathymetric elevation model. The interpolation method, which they chose to create the DTM, is the thin plate spline. The RMSE value for this model amounted to 0.43 m. Despite the large amount of data entered into the model, the RMSE value was high. These examples confirm that the results obtained for the topo-bathymetric surface model in Gdynia are very good.

5. Conclusions

The selection of a terrain modelling method when elaborating data is of major importance [59]. Therefore, the author of the study decided to compare the applied modelling methods that were generated based on the integrated data. The conducted study does not clearly indicate any of

the methods as the selection of the method is also affected by the visualization of the generated model. However, having compared the accuracy measures of the charts and models obtained, it was concluded that for this type of data, the kriging (linear model) method with a preset range of data affecting the value of the interpolated ones was the best. Very good results were also obtained for the NNI method. The application the kriging method requires the user to select the best possible variables that affect the interpolated values. This means that the kriging method will not always generate a very accurate terrain model.

Another important issue that should be addressed when selecting a terrain modelling method is to determine the volume and range of data. Each measurement is characterized by a different volume of data and their distribution. Therefore, it is not possible to conclude that the kriging (linear model) method will perform well with other integrated data.

The article presents an analysis of GRID models generated with different methods. Certainly, in the future, it would be appropriate to apply methods only for the bathymetric data and exclusively for the topographic data. It will then be possible to determine which method performs well for the land, water and combined (land and water) data.

Acknowledgements

This research was funded by the National Centre for Research and Development in Poland, grant number LIDER/10/0030/L-11/19/NCBR/2020. Moreover, this research was funded from the statutory activities of Gdynia Maritime University, grant number WN/PI/2023/03.

References

- [1] Brivio, P. A., Colombo, R., Maggi, M., & Tomasoni, R. (2002). Integration of Remote Sensing Data and GIS for Accurate Mapping of Flooded Areas. *International Journal of Remote Sensing*, 23(3), 429–441. <https://doi.org/10.1080/01431160010014729>
- [2] Brown, D. G., Riolo, R., Robinson, D.T., North, M., & Rand, W. (2005). Spatial Process and Data Models: Toward Integration of Agent-based Models and GIS. *Journal of Geographical Systems*, 7, 25–47. <https://doi.org/10.1007/s10109-005-0148-5>
- [3] Popielarczyk, D., & Templin, T. (2014). Application of Integrated GNSS/Hydroacoustic Measurements and GIS Geodatabase Models for Bottom Analysis of Lake Hancza: The Deepest Inland Reservoir in Poland. *Pure and Applied Geophysics*, 171, 997–1011. <https://doi.org/10.1007/s00024-013-0683-9>
- [4] Abdalla, R. (2016). *Introduction to Geospatial Information and Communication Technology (GeoICT)*. Springer. <https://doi.org/10.1007/978-3-319-33603-9>
- [5] Cao, W., & Wong, M. H. (2007). Current Status of Coastal Zone Issues and Management in China: A Review. *Environmental International*, 33(7), 985–992. <https://doi.org/10.1016/j.envint.2007.04.009>
- [6] Cicin-Sain, B., & Knecht, R. W. (1998). *Integrated Coastal and Ocean Management: Concepts and Practices*. Island Press.
- [7] Lewicka, O., Specht, M., Stateczny, A., Specht, C., Brčić, D., Jugović, A., Widźgowski, S., & Wiśniewska, M. (2021). Analysis of GNSS, Hydroacoustic and Optoelectronic Data Integration Methods Used in Hydrography. *Sensors*, 21(23), 7831. <https://doi.org/10.3390/s21237831>
- [8] Specht, M., Specht, C., Mindykowski, J., Dąbrowski, P., Mańnicki, R., & Makar, A. (2020). Geospatial Modeling of the Tombolo Phenomenon in Sopot Using Integrated Geodetic and Hydrographic Measurement Methods. *Remote Sensing*, 12(4), 737. <https://doi.org/10.3390/rs12040737>

- [9] Kang, M. (2014). Overview of the Applications of Hydroacoustic Methods in South Korea and Fish Abundance Estimation Methods. *Fisheries and Aquatic Sciences*, 17(3), 369–376.
- [10] Makar, A. (2022). Determination of USV's Direction Using Satellite and Fluxgate Compasses and GNSS-RTK. *Sensors*, 22(20), 7895. <https://doi.org/10.3390/s22207895>
- [11] Makar, A. (2008). Method of Determination of Acoustic Wave Reflection Points in Geodesic Bathymetric Surveys. *Annual of Navigation*, 14, 1–89.
- [12] Parente, C., & Vallario, A. (2019). Interpolation of Single Beam Echo Sounder Data for 3D Bathymetric Model. *International Journal of Advanced Computer Science and Applications*, 10(10), 6–13. <https://dx.doi.org/10.14569/IJACSA.2019.0101002>
- [13] Specht, C., Specht, M., & Dabrowski, P. (2017). Comparative Analysis of Active Geodetic Networks in Poland. *Proceedings of the 17th International Multidisciplinary Scientific GeoConference (SGEM 2017)*, Bulgaria. <https://10.5593/sgem2017/22/S09.021>
- [14] Włodarczyk-Sielicka, M., & Stępczyński, A. (2016). Comparison of Selected Reduction Methods of Bathymetric Data Obtained by Multibeam Echosounder. *Proceedings of the 2016 Baltic Geodetic Congress (BGC 2016)*, Poland. <https://doi.org/10.1109/BGC.Geomatics.2016.22>
- [15] Kondo, H., & Ura, T. (2004). Navigation of an AUV for Investigation of Underwater Structures. *Control Engineering Practice*, 12(12), 1551–1559. <https://doi.org/10.1016/j.conengprac.2003.12.005>
- [16] Noureldin, A., Karamat, T.B., & Georgy, J. (2013). *Fundamentals of Inertial Navigation, Satellite-based Positioning and Their Integration*. Springer. <https://doi.org/10.1007/978-3-642-30466-8>
- [17] Specht, M. (2019). Method of Evaluating the Positioning System Capability for Complying with the Minimum Accuracy Requirements for the International Hydrographic Organization Orders. *Sensors*, 19(18), 3860. <https://doi.org/10.3390/s19183860>
- [18] Stępczyński, A. (2016). Radar Water Level Sensors for Full Implementation of the River Information Services of Border and Lower Section of the Oder in Poland. *Proceedings of the 17th International Radar Symposium (IRS 2016)*, Poland. <https://doi.org/10.1109/IRS.2016.7497386>
- [19] Wehr, A., & Lohr, U. (1999). Airborne Laser Scanning – An Introduction and Overview. *ISPRS Journal of Photogrammetry and Remote Sensing*, 54(2–3), 68–82. [https://doi.org/10.1016/S0924-2716\(99\)00011-8](https://doi.org/10.1016/S0924-2716(99)00011-8)
- [20] Williams, R., Brasington, J., Vericat, D., Hicks, M., Labrosse, F., & Neal, M. (2011). Chapter Twenty – Monitoring Braided River Change Using Terrestrial Laser Scanning and Optical Bathymetric Mapping. *Developments in Earth Surface Processes*, 15, 507–532. <https://doi.org/10.1016/B978-0-444-53446-0.00020-3>
- [21] Dąbrowski, P.S., Specht, C., Specht, M., Burdziakowski, P., Makar, A., & Lewicka, O. (2021). Integration of Multi-source Geospatial Data from GNSS Receivers, Terrestrial Laser Scanners, and Unmanned Aerial Vehicles. *Canadian Journal of Remote Sensing*, 47(4), 621–634. <https://doi.org/10.1080/07038992.2021.1922879>
- [22] Erena, M., Atenza, J. F., García-Galiano, S., Domínguez, J. A., & Bernabé, J. M. (2019). Use of Drones for the Topo-bathymetric Monitoring of the Reservoirs of the Segura River Basin. *Water*, 11(3), 445. <https://doi.org/10.3390/w11030445>
- [23] Lubczonek, J., Kazimierski, W., Zaniewicz, G., & Lacka, M. (2022). Methodology for Combining Data Acquired by Unmanned Surface and Aerial Vehicles to Create Digital Bathymetric Models in Shallow and Ultra-shallow Waters. *Remote Sensing*, 14(1), 105. <https://doi.org/10.3390/rs14010105>

- [24] Specht, C., Świtalski, E., & Specht, M. (2017). Application of an Autonomous/Unmanned Survey Vessel (ASV/USV) in Bathymetric Measurements. *Polish Maritime Research*, 24(3), 36–44. <https://doi.org/10.1515/pomr-2017-0088>
- [25] Specht, M., Specht, C., Szafran, M., Makar, A., Dąbrowski, P., Lasota, H., & Cywiński, P. (2020). The Use of USV to Develop Navigational and Bathymetric Charts of Yacht Ports on the Example of National Sailing Centre in Gdańsk. *Remote Sensing*, 12(16), 2585. <https://doi.org/10.3390/rs12162585>
- [26] Lewicka, O., Specht, M., & Specht, C. (2022). Assessment of the Steering Precision of a UAV along the Flight Profiles Using a GNSS RTK Receiver. *Remote Sensing*, 14(23), 6127. <https://doi.org/10.3390/rs14236127>
- [27] Golden Software LLC. (2023, 28 April). *Surfer® User's Guide*. <https://downloads.goldensoftware.com/guides/Surfer20UserGuide.pdf>
- [28] Council of Ministers of the Republic of Poland (2012). *Ordinance of the Council of Ministers of 15 October 2012 on the National Spatial Reference System*. Council of Ministers of the Republic of Poland. (in Polish)
- [29] Pham, H. (2019). A New Criterion for Model Selection. *Mathematics*, 7(12), 1215. <https://doi.org/10.3390/math7121215>
- [30] Willmott, C. J., & Matsuura, K. (2005). Advantages of the Mean Absolute Error (MAE) over the Root Mean Square Error (RMSE) in Assessing Average Model Performance. *Climate Research*, 30(1), 79–82. <http://dx.doi.org/10.3354/cr030079>
- [31] Di Bucchianico, A. (2008). Coefficient of Determination (R^2). In Ruggeri, F., Kenett, R. S., & Faltin, F. W. (Eds.). *Encyclopedia of Statistics in Quality and Reliability*. John Wiley & Sons, Inc. <http://doi:10.1002/9780470061572>
- [32] Szot, T., Specht, C., Specht, M., & Dabrowski, P. S. (2019). Comparative Analysis of Positioning Accuracy of Samsung Galaxy Smartphones in Stationary Measurements. *PLoS ONE*, 14(4), e0215562. <https://doi.org/10.1371/journal.pone.0215562>
- [33] Makar, A., Specht, C., Specht, M., Dąbrowski, P., Burdziakowski, P., & Lewicka, O. (2020). Seabed Topography Changes in the Sopot Pier Zone in 2010–2018 Influenced by Tombolo Phenomenon. *Sensors*, 20(21), 6061. <https://doi.org/10.3390/s20216061>
- [34] Lu, G. Y., & Wong, D. W. (2008). An Adaptive Inverse-Distance Weighting Spatial Interpolation Technique. *Computers & Geosciences*, 34(9), 1044–1055. <https://doi.org/10.1016/j.cageo.2007.07.010>
- [35] Ohlert, P.L., Bach, M., & Breuer, L. (2022). Accuracy Assessment of Inverse Distance Weighting Interpolation of Groundwater Nitrate Concentrations in Bavaria (Germany). *Environmental Science and Pollution Research*, 30, 9445–9455. <https://doi.org/10.1007/s11356-022-22670-0>
- [36] Bartier, P. M., & Keller, C. P. (1996). Multivariate Interpolation to Incorporate Thematic Surface Data Using Inverse Distance Weighting (IDW). *Computers & Geosciences*, 22(7), 795–799. [http://dx.doi.org/10.1016/0098-3004\(96\)00021-0](http://dx.doi.org/10.1016/0098-3004(96)00021-0)
- [37] Davis, J. C. (2002). *Statistics and Data Analysis in Geology*. John Wiley & Sons, Inc.
- [38] Basso, K., De Avila Zingano, P. R., & Dal Sasso Freitas, C. M. Interpolation of Scattered Data: Investigating Alternatives for the Modified Shepard Method. *Proceedings of the XII Brazilian Symposium on Computer Graphics and Image Processing*, Brazil. <https://doi.org/10.1109/SIBGRA.1999.805606>
- [39] Malvić, T., Ivšiniović, J., Velić, J., Sremac, J., & Barudžija, U. (2020). Application of the Modified Shepard's Method (MSM): A Case Study with the Interpolation of Neogene Reservoir Variables in Northern Croatia. *Stats*, 3(1), 68–83. <https://doi.org/10.3390/stats3010007>

- [40] Renka, R. J. (1988). Multivariate Interpolation of Large Sets of Scattered Data. *ACM Transactions on Mathematical Software*, 14(2), 139–148. <https://doi.org/10.1145/45054.45055>
- [41] Cueto, E., Sukumar, N., Calvo, B., Martínez, M.A., Cegoñino, J., & Doblaré, M. (2003). Overview and Recent Advances in Natural Neighbour Galerkin Methods. *Archives of Computational Methods in Engineering*, 10, 307–384. <https://doi.org/10.1007/BF02736253>
- [42] Sibson, R. (1981). A Brief Description of Natural Neighbor Interpolation. In Barnett, V. (Ed.). *Interpreting Multivariate Data* (pp. 21–36). John Wiley & Sons, Inc.
- [43] Fanchi, J. R. (2018). Chapter 2 — Geological Modeling. In Fanchi, J. R. (Ed.). *Principles of Applied Reservoir Simulation* (pp. 9–33). Gulf Professional Publishing.
- [44] Journel, A. G., & Huijbregts, Ch. J. (1978). *Mining Geostatistics*. Cambridge.
- [45] Rodzinska, O., Perovych, I., Perovych, L., & Ludchak, O. GIS Technologies for Integrating Cartographic Materials into a Single Coordinate System. *Proceedings of the 18th International Conference on Geoinformatics – Theoretical and Applied Aspects*, Ukraine. <https://doi.org/10.3997/2214-4609.201902042>
- [46] Jiménez-Jiménez, S. I., Ojeda-Bustamante, W., Marcial-Pablo, M. d. J., & Enciso, J. (2021). Digital Terrain Models Generated with Low-cost UAV Photogrammetry: Methodology and Accuracy. *ISPRS International Journal of Geo-Information*, 10(1), 285. <https://doi.org/10.3390/ijgi10050285>
- [47] Nikolakopoulos, K.G., Lampropoulou, P., Fakiris, E., Sardelianos, D., & Papatheodorou, G. (2018). Synergistic Use of UAV and USV Data and Petrographic Analyses for the Investigation of Beachrock Formations: A Case Study from Syros Island, Aegean Sea, Greece. *Minerals*, 8(11), 534. <https://doi.org/10.3390/min8110534>
- [48] Anderson, T. W., & Darling, D. A. (1954). A Test of Goodness of Fit. *Journal of the American Statistical Association*, 49(268), 765–769.
- [49] Kolmogorov, A. (1933). Sulla Determinazione Empirica di una Legge di Distribuzione. *Giornale dell'Istituto Italiano degli Attuari*, 4(1), 83–91. (in Italian)
- [50] Pearson, K. (1900). On the Criterion that a Given System of Deviations from the Probable in the Case of a Correlated System of Variables is Such that it Can be Reasonably Supposed to Have Arisen from Random Sampling. *The London, Edinburgh, and Dublin Philosophical Magazine and Journal of Science*, 50(302), 157–175. <https://doi.org/10.1080/14786440009463897>
- [51] Smirnov, N. (1948). Table for Estimating the Goodness of Fit of Empirical Distributions. *The Annals of Mathematical Statistics*, 19(2), 279–281. <https://doi.org/10.1214/aoms/1177730256>
- [52] Specht, M. (2021). Consistency Analysis of Global Positioning System Position Errors with Typical Statistical Distributions. *Journal of Navigation*, 74(6), 1201–1218. <https://doi.org/10.1017/S0373463321000485>
- [53] Specht, M. (2021). Consistency of the Empirical Distributions of Navigation Positioning System Errors with Theoretical Distributions – Comparative Analysis of the DGPS and EGNOS Systems in the Years 2006 and 2014. *Sensors*, 21(1), 31. <https://doi.org/10.3390/s21010031>
- [54] Specht, M. (2021). Determination of Navigation System Positioning Accuracy Using the Reliability Method Based on Real Measurements. *Remote Sensing*, 13(21), 4424. <https://doi.org/10.3390/rs13214424>
- [55] Specht, M. (2022). Experimental Studies on the Relationship Between HDOP and Position Error in the GPS System. *Metrology and Measurement Systems*, 29(1), 17–36. <http://dx.doi.org/10.24425/mms.2022.138549>

O. Lewicka: METHOD FOR ACCURACY ASSESSMENT OF TOPO-BATHYMETRIC SURFACE MODELS...

- [56] Lubczonek, J., Włodarczyk-Sielicka, M., Lacka, M., & Zaniewicz, G. (2021). Methodology for Developing a Combined Bathymetric and Topographic Surface Model Using Interpolation and Geodata Reduction Techniques. *Remote Sensing*, 13(21), 4427. <https://doi.org/10.3390/rs13214427>
- [57] Genchi, S. A., Vitale, A. J., Perillo, G. M. E., Seitz, C., & Delrieux, C. A. (2020). Mapping Topobathymetry in a Shallow Tidal Environment Using Low-cost Technology. *Remote Sensing*, 12(9), 1394. <https://doi.org/10.3390/rs12091394>
- [58] Gesch, D., & Wilson, R. (2001). Development of a Seamless Multisource Topographic/Bathymetric Elevation Model of Tampa Bay. *Marine Technology Society Journal*, 35(4), 58–64. <https://doi.org/10.4031/002533201788058062>
- [59] Stateczny, A. (2000). The Neural Method of Sea Bottom Shape Modelling for the Spatial Maritime Information System. In Brebbia, C.A., & Olivella, J. (Eds.). *Maritime Engineering and Ports II* (pp. 251–259). WIT Press. <https://doi.org/10.2495/PORTS000221>



Oktawia Lewicka works at Gdynia Maritime University as an Assistant at the Department of Geodesy and Oceanography and also she is a contractor for the National Centre for Research and Development (Poland) grant entitled “Innovative Autonomous Unmanned Bathymetric Monitoring System for Shallow Waterbodies”. Her overall scientific output comprises a total of 19 peer-reviewed publications, including 17 articles in JCR-listed journals. Her research interests are focused on

geoinformatics and oceanography.